FOCUSING INDUCTION ACCELERATOR

J. Bernardes
Naval Surface Weapons Center
Dahlgren, Virginia 22448

Abstract

This paper describes a unique induction accelerator that simultaneously axially accelerates and radially compresses conic-section-shaped, sheet-copper rings. The result of this process is an axially flying, compact slug.

A description of the experimental set-up and of the testing of this device is presented. Special attention is given to the drive-coil design, which includes a barrel, and to the investigation of the ring-forming process using high-speed photography.

Introduction

A significant acceleration is experienced by a conducting ring if it is both coaxial and adjacent to an electric coil when the coil is energized by a current pulse. This acceleration is produced by a Lorentz force acting on the ring which is the result of the interaction between the magnetic field launched from the coil, at the ring's surface, and the circumferential current induced in the ring by this same field as it diffuses into the ring material. The above is the basis for the operation of induction accelerators.

The direction in which the ring is accelerated depends on the relative arrangement of the ring and the drive-coil as depicted in Figure 1. Figure 1a depicts a geometry that is typical of reaction engine devices which accelerate a flat ring axially. Figure 1b depicts a geometry typical of flux compression and metal-forming devices which drive the tubular ring-workpiece radially. The Focusing Induction Accelerator (FIA) employs a drive assembly geometry that is a combination of the above two geometries. In the FIA the ring has a conic-section shape which mates to an angled surface on the drive coil as is shown in Figure 1c. This geometry produces a force on the ring that has both a radial and an axial component. This force simultaneously axially accelerates and radially deforms the ring into a compact mass. The final result of this process is an axial-flying slug.

The idea for this device was conceived by Rose and Fitch [1] in 1982. This paper is derived from subsquent investigation and engineering of this concept towards a high-velocity small caliber accelerator.

Accelerator

The FIA consists of two capacitor banks and a drive-coil assembly connected in series through a pneumatically driven closing switch. A view of the device, in which the main components are indicated, is shown in Figure 2. The twelve capacitors that make-up the two banks are stacked on their sides, around a mechanically floating section that supports the drive-coil assembly and absorbs the recoil forces transmitted from the drive-coil. The floating section rests on wheels, and it is supported from the rear by an air filled rubber bladder. Recoil distances of the order of 0.5 cm were normally measured. The drive-coil is electrically connected to the stationary part of the device through flexible copper braid. The pneumatic switch is located directly below the flanged leads of the coil. The reason for this arrangement of components was to minimize stray inductance - which was measured to be 0.4 μH.

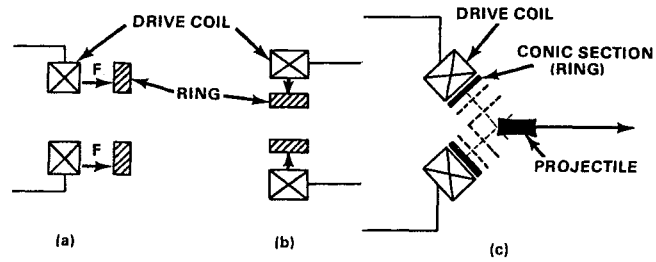

Fig. 1. Illustration of three coil-ring geometries indicating the direction of ring motion.

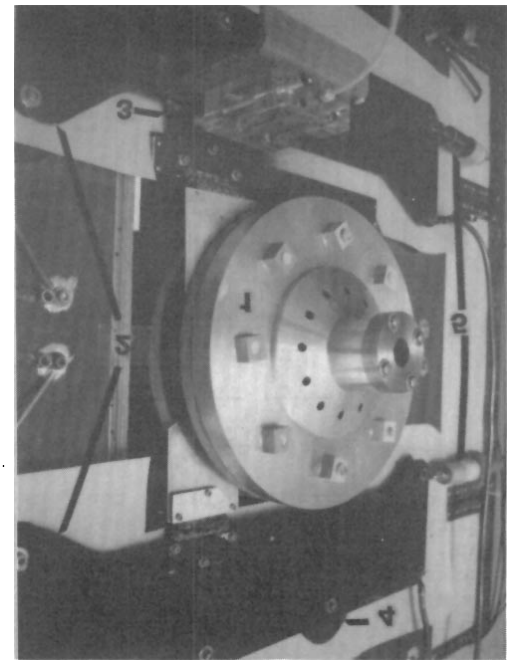

Fig. 2. Photo of the FIA indicating some of its main components: (1) drive-coil assembly, (2) HV terminals of cap. banks, (3) Pneumatic switch, (4) Rogowski coil, and (5) voltage probes.

Each capacitor bank has a capacitance of 828 μF and is rated at 20 kV and 300 kA. During operation, only one bank is initially charged. When the switch is closed the voltage across each bank rings with respect to a voltage level that is equal to one-half the charge voltage - without ever going negative.

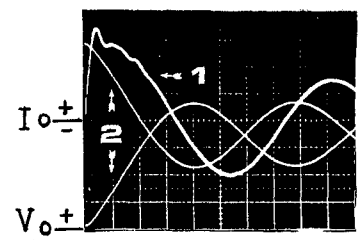

Fig. 3. Typical waveforms of: (1) drive-coil current and (2) capacitor banks voltages.

Figure 3 shows typical time traces of the capacitor banks voltages and the coil current. The voltage and

Report Documentation Page

Form Approved
OMB No. 0704-0188

1. REPORT DATE	2. REPORT TYPE	3. DATES COVERED
JUN 1987	**N/A**	**-**

4. TITLE AND SUBTITLE	5a. CONTRACT NUMBER
Focusing Induction Accelerator	5b. GRANT NUMBER
	5c. PROGRAM ELEMENT NUMBER
6. AUTHOR(S)	5d. PROJECT NUMBER
	5e. TASK NUMBER
	5f. WORK UNIT NUMBER
7. PERFORMING ORGANIZATION NAME(S) AND ADDRESS(ES) **Naval Surface Weapons Center Dahlgren, Virginia 22448**	8. PERFORMING ORGANIZATION REPORT NUMBER
9. SPONSORING/MONITORING AGENCY NAME(S) AND ADDRESS(ES)	10. SPONSOR/MONITOR'S ACRONYM(S)
	11. SPONSOR/MONITOR'S REPORT NUMBER(S)

12. DISTRIBUTION/AVAILABILITY STATEMENT
Approved for public release, distribution unlimited

13. SUPPLEMENTARY NOTES
See also ADM002371. 2013 IEEE Pulsed Power Conference, Digest of Technical Papers 1976-2013, and Abstracts of the 2013 IEEE International Conference on Plasma Science. Held in San Francisco, CA on 16-21 June 2013. U.S. Government or Federal Purpose Rights License.

14. ABSTRACT
This paper describes a unique induction accelerator that simultaneously axially accelerates and radially compresses conic-section-shaped, sheet-copper rings. The result of this process is an axially flying, compact slug. A description of the experimental set-up and of the testing of this device is presented. Special attention is given to the drive-coil design, which includes a barrel, and to the investigation of the ring-forming process using high-speed photography.

15. SUBJECT TERMS

16. SECURITY CLASSIFICATION OF:			17. LIMITATION OF ABSTRACT	18. NUMBER OF PAGES	19a. NAME OF RESPONSIBLE PERSON
a. REPORT	b. ABSTRACT	c. THIS PAGE			
unclassified	**unclassified**	**unclassified**	**SAR**	**4**	

current oscilate at the same frequency (determined by the effective inductance and capacitance of the circuit), but 90-degrees out of phase. The frequency is initially high due to the presence of the ring in the coupling region of the coil. Once the ring leaves the coupling region the waveform settles to a constant frequency. A more detailed description of this circuit, including a computer simulation, is presented in reference 2. There were two reasons for choosing this circuit: (1) to prevent voltage reversal across the capacitors - this prevents premature capacitor failure, and (2) to possibly implement an energy recovery scheme that would operate an opening switch at the first current zero crossing (a perceived feasible time to operate an opening switch) thereby recovering, in the initially uncharged bank, a large percentace of the energy not used in the acceleration process.

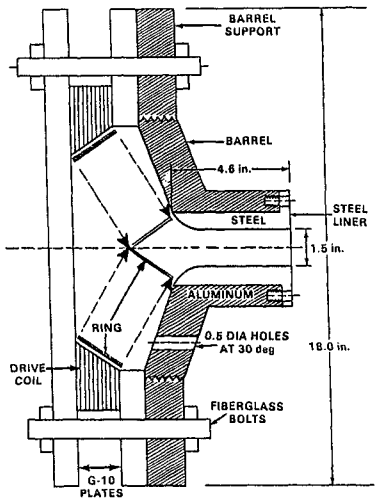

Fig. 4. Cross-section view of drive-coil assembly.

The drive coil assembly (Figure 4) consists of the following parts: a drive-coil that uses a Bitter Helix design, approximately 20 cm in inner diameter, with its inner surface machined at an angle relative to the coil axis; a conic-section shaped, sheet-copper ring that mates to the coils angled surface; two G-10 plates that contain the coil; and a short barrel that screws into a circular aluminum plate that in turn is secured to the assembly by the same fiberglass bolts that contain the G-10 plates. Photographs of these different parts are shown in Figure 5.

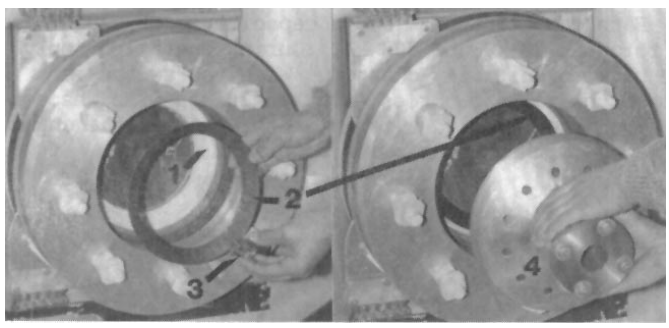

Fig. 5. Photos showing the different components of the drive-coil assembly: (1) the drive-coil, (2) the ring, (3) the slug projectile, and (4) the barrel.

The helix drive-coil was initially fabricated by welding into a stack, flat, washer-like, turns (made from 1/8 in. aluminum plate). Because of problems with the welds joints separating, the coil was later machined from a solid piece of aluminum . The conic-section rings ranged in thickness from 5 to 43 mils, ranged in width from 7.1 to 3.3 cm, which resulted in masses that ranged from 20 to 335 g. The ring had the same dimensions as the drive-coil's angled surface in order to maximize the magnetic coupling. Originally, the rings included a solder seam in their assembly. This seam provided an undesirable mass discontinuity. The later rings were stamped from a solid sheet of copper. Aside from the steel liner, the barrel and its supporting ring are made of aluminum. The breech of the barrel is located near the focal point of the collapsing ring (see Figure 4) which is determined by the angle of the coil. Circumferential holes were added to the forming chamber to provide an air inlet during the forming process. The barrel bore-diameter and length are respectively 1.5 and 4.6 inches. The bore diameter was designed to provide a loose fit for all projectile diameters.

Diagnostics

The diagnostics for this experiment include measurements of the coil current, the capacitor banks voltages, and the projectile velocity - as well as high speed photography of the ring forming and flight. The current was measured with a passively integrated, shielded Rogowski coil with a sensitivity of 10 MV/A, and the voltages were measured using 1000:1 Tektronix probes. A sample oscillograph of these measurements is shown in Figure 3. The voltage traces include an erroneous phase shift that was introduced by the probes. The projectile velocity was measured with a four light-beam set-up, with each beam separated by one foot. The beams are generated by a bulb-lens arrangement with their presence sensed by four photodetector circuits via four fiber optic cables. The fiber optics are used to remove the electronics from the noisy experiment environment. Each photodetector circuit produces a different voltage level between 0 and 5 volts. The four outputs of the detector circuits are fed into an adder circuit before being recorded on an oscillogaph. The interruption of the beams produces a series of pulses of different amplitude on the oscillograph (individualizing each beam) from which the velocity can be extracted, since the beam separation is known. This scheme was designed to measure velocities of projectiles that partly fragment or that may be accompanied by debris. The high-speed photography set-up consists of a movie camera operating at 7000 frames/sec and a disposable mirror in an arrangement shown in Figure 6.

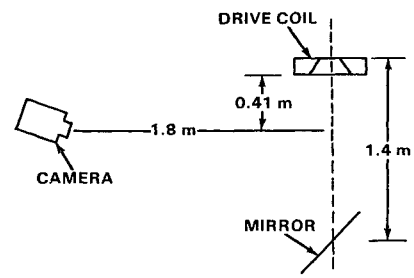

Fig. 6. Arrangement of high-speed photography set-up.

This set-up provides both front and side views of the event. In addition, the projectile velocity is obtained by placing two vertical stripes, a known distance apart (distance adjusted for lense distortion), in the background of the side view and then counting the number of frames it takes for the projectile to cross

that distance. A sample of the series of photos obtained with this set-up are shown in Figures 7 and 8. Figure 7 shows the split image frame discussed above. The coil is located on the left while the mirror image of the front-view of the coil is on the right. The two stripes in the background represent a distance of one foot. Figure 8 is a close-up of the mirror image that shows the detailed progression of the ring forming process.

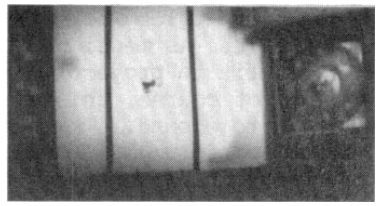

Fig. 7. Split-view high-speed photo. The coil is on the left, the coil's front view (mirror image) is on the right, and the flying projectile is in the center.

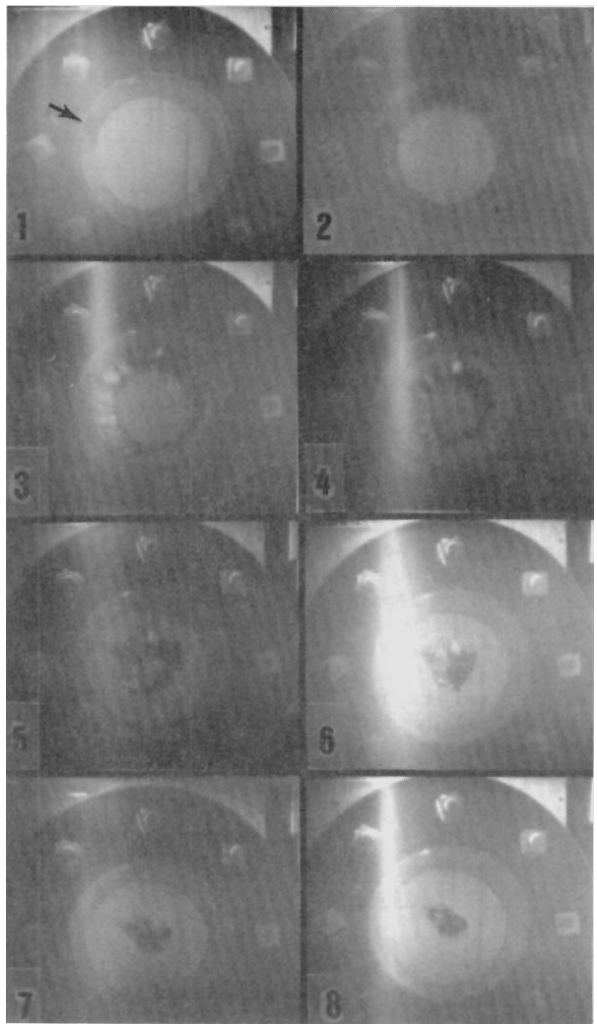

Fig. 8. High-speed photos showing a detailed progression of the ring-forming-process.

Experiments

The main goal of these experiments was to generate the highest projectile velocity possible, within the limits of the available electrical energy (~150 KJ), and at the same time produce a tightly formed projectile. It quickly became evident that the biggest challenge would be maintaining the integrity of the drive-coil and projectile. Damage to the coil occurred as a result of inter-turn breakdown caused by insulation failure. This was due to physical damage to the insulation or plain electrical stresses. This problem was controlled by: (1) building a recoil mechanism, (2) eliminating weld joints, and (3) insulating the coil with teflon tape. A description of the different drive-coils tested and their performance is presented in the "Drive Coils" subsection. Each ring, depending on its thickness, was found to begin fragmenting when a certain initially stored electrical energy was exceeded. This energy level increased with thickness as illustrated in Figure 9, which shows a series of recovered projectiles that are arranged according to ring thickness and charge energy. This figure also indicates that there exists an optimum force for each ring thickness that produces a compact projectile. Throughout the course of the experiments significant improvements were made in the ring forming process at modest velocities (100 to 200 m/sec - axial), but as the velocity/charge-energy was increased it became impossible to keep the ring from fragmenting. Two fundamental problems with this acceleration process became evident: (1) the short distance in which the ring must be accelerated, and (2) the significant heating that occurs in the ring due to resistive loses. The acceleration distance was measured by Bondaletov [3] to be 0.1-0.15D, where D is the ring diameter. In our case this distance is 2 to 3 cm (D=20cm). The forces required to accelerate the ring to significant velocities quickly exceed the strength of the ring material. This is compounded by heating that, at high currents, can melt the ring. Further details of the measured and observed ring dynamics is presented in the "Ring" subsection.

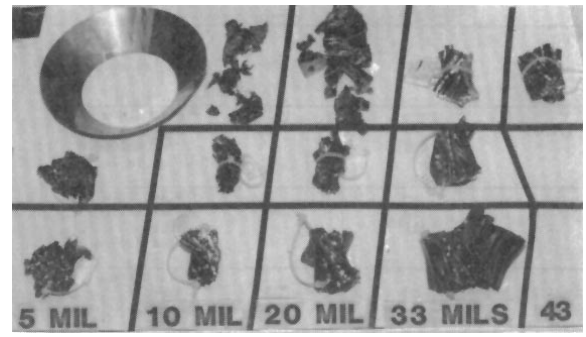

Fig. 9. Series of recovered projectiles arranged according to ring thickness and initially stored electrical energy. Unformed ring is shown in upper left corner.

Drive-coil

Table 1 summarizes, in chronological order, the main points of the six drive coils that were tested. This table lists: (1) the coil dimensions (see figure below the table), the number of turns and the inductance of each coil, the peak voltage and current where each coil failed (also the highest voltage before failure), and comments on the construction and failure mode. Coils #1 - #4 had welded turns. At currents near 80 kA the weld joints separated causing the coils to fail. The failure is suspected to have been caused by mechanical stresses that fractured the weld which then led to arcing and consequently destruction of the weld region. This problem was solved in coil #5 by milling the coil from a single piece of aluminum. Coils #1 & #2 were insulated by placing mylar sheets in between the turns, and then potting the coil in an epoxy compound (castall). This proved unsuccessful at

voltages much greater then 10 kV - breakdown occurred along the angled surface which relied mainly on the potting material for insulation. In this case, the failure is suspected to have been caused by mechanical stresses that cracked the potting material which then led to arcing. A solution to this problem was to insulate each turn with several layers of teflon tape. A continuous taping was accomplished by stretching the helix with spacers that were high enough to allow a roll of tape to fit in between the windings. Teflon was chosen as the insulator because of its high dielectric strength, as well as its good mechanical and temperature properties. Coil #5 was the most successful in terms of surviving the highest voltages and producing the best formed projectiles. although its insulation failed before reaching 20 kV, the failure appeared to have been caused by punctures to the insulator by ring fragments rebounding from the barrel structure. In coil #6 the drive angle was increased to 61-degrees to reduce the radial component of the accelerating force, which is believed to be the main reason for severe ring fragmentation observed with coil #5 at voltages above 12 kV. For example at 14 kV most of the 5 mil ring was plated, in granular form on the orifice of the barrel. Coil #6 had single turn because of the perceived difficulty in supporting a multiturn coil with a shalow angle. Its low inductance (comparable to the stray inductance) made it inefficient, but it did survive at 20 kV/~400 kA. With this coil, the inner diameter region of the ring was driven faster, causing the ring to turn inside-out before collapsing.

Table 1. Summary of drive-coils performance

COIL DIM.	NO.OF TURNS/ INDUCTANCE	PEAK VOLTS [BEFORE FAILURE]	PEAK CURRENT	COMMENTS
(#1.) D=17.8cm L=6.4cm θ=45deg	12/36.1μH	12KV [10KV]	~36KA	-Turns welded -No recoil mech. -Castal/mylar ins. -Insul. failure
(#2.) D=17.7 L=3.9 θ=45	6/7.3	10 [7]	78	-Recoil mech. -Same as above
(#3.) D=18.1 L=3.8 θ=38	7/13.1	15 [10]	78	-Teflon insul. (3x3mil layers) -Turns welded -Welds failed
(#4.) D=17.8 L=5.1 θ=32.3	7/13.7	12 [11]	66	-Teflon insul. (3x3mil+2x6mil) -Barrel -Welds failed
(#5.) D=16.7 L=3.3 θ=45	4/3.7	19 [14]	~190	-Teflon insul. (3x6mil) -No welds -Barrel -Insul. failure
(#6.) D=2.5 L=7.14 θ=61	1/~0.4	[20]	~400	-Teflon Ins. -Barrel -No failure

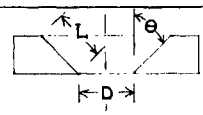

Ring

Maintaining symmetry in the collapse of the ring is important in achieving a compact crush of the ring. Several sources of asymmetries were identified: mass discontinuities in the ring, non-uniform magnetic field in the feed region that leads to a non-uniform force distribution, non-uniform coil-angle, and nonuniform ring-coil separation. Figure 8 shows the effect of the most obvious of these effects, the ring mass discontinuity introduced by the soldered seam. The dark mark on the ring indicates the location of the discontinuity which lags the rest of the ring. As mentioned before this problem was corrected by stamping the rings. Asymmetries dictate the projectile shape up to a certain accelerating force - determined by the ring thickness. Beyond this force, the ring collapses as a unit to its focal point, but then rebounds, and if the force is large enough it fragments. In all cases observed with high-speed photography no evidence of ring separation was detected during the collapse stage. This was the reason for building a barrel. By placing the orifice of the barrel at the focal point of the collapse, the rebounding forces were contained and the shape of the projectile was dramatically improved. Figure 5 shows a projectile that was formed with the aid of the barrel. The barrel raised the drive-force where fragmentation occurs but did not stop it. As mentioned before, the barrel provided a loose fit to projectile in order to minimize friction, but, of course, this also provided room for the projectile to expand. The barrel liner was designed to be easily replaced in order to change barrel-bore diameter to possibly extrude the projectile, but these experiments were never performed.

Table 2. Measurements from a typical series of shots

THICKNESS [MASS]	PEAK VOLTAGE	PEAK CURRENT	NORMAL VEL./ AXIAL VEL.	DRIVE EFF.
5mils [38.1g]	7.5KV	33KA	378/--- m/sec	23.4%
10mils [78.1]	6.5	39	327/110	48
*[86.8]	5.6	31.2	256/99.8	45
[76.2]	4.6	28.8	226/---	44.4
15mils [114.6]	5.6	36	267/97	62.9
20mils [54.6]	6.5	42	268/95.5	63.5
32mils	6.6	45.6	227/---	66.6

* pieces of copper of the same weight as seam-overlap soldered at 90-deg increments from seam

Table 2 lists a series of the measured parameters for a typical cross-section of shots (using coil #4). The table lists: (1) ring thickness and mass, peak capacitor-bank voltage, coil current, normal and axial ring/projectile velocity, and drive efficiency. The velocities were obtained from the high-speed movies - the normal from the front-view angle and the axial from the side-view. The normal velocity is the velocity of the collapsing ring normal to the drive-coil's angled surface. This was obtained by measuring the change in diameter of the collapsing ring between frames, and then calculating the travelled normal distance. The drive efficiency is the ratio of the rings kinetic energy, based on the normal velocity, to one-half the initially stored energy. Due to the nature of the circuit used, one-half of the energy is always recovered - one-quarter in each capacitor bank.

References

1. M. F. Rose, O. Fitch, Electromagnetic Induction Method and Apparatus for Collapsing and Propelling a Deformable Workpiece, Navy Patent Case 67-217, Feb. 1985

2. J. S. Bernardes, S. Merryman, Parameter Analysis of a Single Stage Induction Mass Driver, Fifth IEEE Pulsed Power Conference Proceedings, June 1985

3. V. N. Bondaletov, E. N. Ivanov, Ultrahigh Axial Acceleration of Conducting Rings, Sov. Phys. Tech. Phys., Vol. 22, No. 2, Feb. 1977